



Hydrogen-bond density controlled sub- T_g annealing peaks in fast-scanning-chip calorimeter heating scans of non-crystallized aliphatic polyamides

René Androsch^{a,*}, Christoph Schick^b

^a Interdisciplinary Center for Transfer-oriented Research in Natural Sciences, Martin Luther University Halle-Wittenberg, Hoher Weg 7a, 06120 Halle/Saale, Germany

^b Institute of Physics and Competence Centre CALOR, University of Rostock, 18051 Rostock, Germany

ARTICLE INFO

Keywords:

Polyamides
Physical aging
Glass relaxation
Fast scanning calorimetry
Annealing peaks

ABSTRACT

A series of aliphatic polyamides (PAs) including PA 6, PA 6.6, PA 6.10, PA 6.12, PA 11, and PA 12 has been subjected to physical aging and analyzed regarding changes of structure during annealing at temperatures around 50 to 100 K below the glass transition temperature (T_g) for periods up to few hours, employing fast scanning chip calorimetry (FSC). Annealing the amorphous glass of non-crystallized samples at such low temperatures produces endothermic sub- T_g annealing peaks at slightly higher temperature in subsequently recorded FSC heating scans, scaling in area with the time of annealing for a given annealing temperature. Variation of the annealing temperature furthermore indicates that the underlying process of structure-change slows down with decreasing annealing temperature but not disappears even 100 K below T_g . Most important, comparison of the behavior of the various PAs investigated reveals a distinct effect of the chemical structure such that the amount of structure-reorganization (glass relaxation and/or ordering) in a pre-defined period of time reduces with decreasing methylene-group sequence-length between amide groups. It appears that the amide-group concentration in the chains, which determines the density of the hydrogen-bond network to neighbored molecular segments, controls/restricts the re-arrangements of sub-nm sized molecular units.

1. Introduction

Cooling amorphous polymers to below the glass transition temperature T_g causes formation of initially thermodynamically unstable glasses of relatively high enthalpy and specific volume. This is caused by the decrease of molecular mobility of the segments below a critical value on lowering the temperature, needed for cooperative segmental mobility (often called segmental- or α -relaxation), being fast only above T_g and quickly fading in a temperature window of 30–50 K below T_g [1,2]. While the typical time scale to adopt a temperature-dependent quasi-equilibrium structure is of the order of magnitude of picoseconds in the liquid state, [3] in the glassy state the relaxation time increases with the difference between the glass-annealing temperature and T_g from, roughly, milliseconds to even millions of years [4–7]. The quasi-equilibrium state is then defined by the free volume and enthalpy of the corresponding liquid at identical temperature, with its approach requiring changes of conformations of covalent bonds (also called large-amplitude motion) [8]. Typical experiments for quantification the

glass-relaxation kinetics include in a first step the vitrification of the liquid phase at a specific cooling rate, which controls the (in-)stability of the obtained glass, being higher on faster cooling. Then, in the next step, either the time-dependence of the decrease of the specific volume is directly measured, or the decrease of the enthalpy is followed indirectly, by analysis of enthalpy-recovery peaks in calorimeter heating scans recorded after a specific glass-annealing history [9–11]. The analysis of the rather slow decrease of the free volume within the glass- α -relaxation process at temperatures up to a few ten K below T_g , again, involving slow cooperative mobility of nm-sized units, is of great economic/engineering importance as it affects ultimate properties of polymeric materials, for example leading to embrittlement or affecting diffusion, also called physical aging, [12–16] with similar property changes reported e.g. for metallic glasses [17,18].

With decreasing temperature in the glassy state, related to the further decrease of the free volume, cooperative segmental mobility diminishes, and only smaller structural units remain mobile and contribute to glass relaxation by local non-cooperative molecular

* Corresponding author.

E-mail address: rene.androsch@iw.uni-halle.de (R. Androsch).

<https://doi.org/10.1016/j.tca.2025.179997>

Received 4 March 2025; Received in revised form 31 March 2025; Accepted 2 April 2025

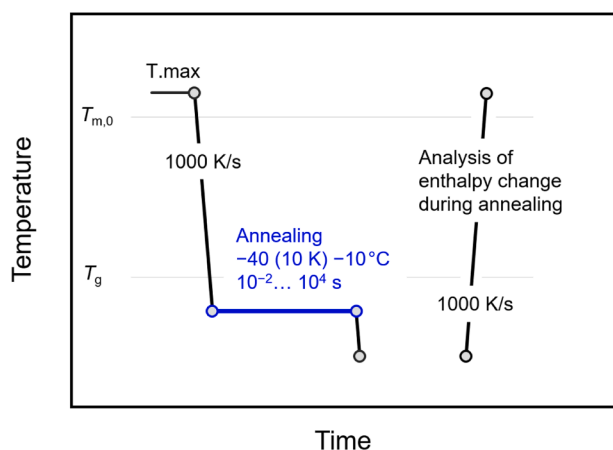
Available online 4 April 2025

0040-6031/© 2025 The Author(s). Published by Elsevier B.V. This is an open access article under the CC BY license (<http://creativecommons.org/licenses/by/4.0/>).

Table 1List of polyamide samples including source, grade, chemical structure of repeat unit, CH₂/NH-CO number ratio, and glass transition temperature T_g .

	Source/grade	Chemical structure of repeat unit	CH ₂ /NH-CO Number ratio	T_g (°C) (*)
PA 6	BASF Ultramid B27	$\left[\text{N} - (\text{CH}_2)_5 - \text{C} \right]_n$ $\begin{array}{c} \\ \text{H} \\ \\ \text{O} \end{array}$	5/1	57.5
PA 6.6	DuPont Zytel 101	$\left[\text{NH} - (\text{CH}_2)_6 - \text{NH} - \text{C} - (\text{CH}_2)_4 - \text{C} \right]_n$ $\begin{array}{c} \\ \text{O} \\ \\ \text{O} \end{array}$	10/2	57.5
PA 6.10	DuPont Zytel 3060	$\left[\text{NH} - (\text{CH}_2)_6 - \text{NH} - \text{C} - (\text{CH}_2)_8 - \text{C} \right]_n$ $\begin{array}{c} \\ \text{O} \\ \\ \text{O} \end{array}$	14/2	45
PA 6.12	Sigma-Aldrich	$\left[\text{NH} - (\text{CH}_2)_6 - \text{NH} - \text{C} - (\text{CH}_2)_{10} - \text{C} \right]_n$ $\begin{array}{c} \\ \text{O} \\ \\ \text{O} \end{array}$	16/2	40
PA 11	Arkema Rilsan BESNO TL	$\left[\text{N} - (\text{CH}_2)_{10} - \text{C} \right]_n$ $\begin{array}{c} \\ \text{H} \\ \\ \text{O} \end{array}$	10/1	40
PA 12	EMS-Grivory Grilamid L20	$\left[\text{N} - (\text{CH}_2)_{11} - \text{C} \right]_n$ $\begin{array}{c} \\ \text{H} \\ \\ \text{O} \end{array}$	11/1	40

(*) Estimates based on FSC cooling scans using a rate of 1000 K/s.

**Fig. 1.** Temperature-time profile for analysis of the change of structure deep in the glassy state of polyamides.

motion, often denoted as β -relaxations [19,20]. Their apparent activation energy is lower than for the α -relaxation process, thus being activated at lower temperature, and the relaxation times, at a given temperature, are much shorter. For aliphatic polyamides, being in focus in the present work, α - and β -relaxations are associated with cooperative motions of larger segments/units and the mobility of amide groups, respectively, and occur at common laboratory time scales at temperatures of around 50 and -40 °C; also the motion of methylene groups (denoted as γ -relaxation) is detected at around -120 °C [21,22]. These information were obtained by dynamic-mechanical or dielectric analyses, allowing their filtering by frequency variation of the perturbation, based on the largely different relaxation times, while the assignment of the β - and γ -relaxations to specific structural units was done by systematic variation of the concentration of amide groups in the repeat unit of the macromolecular chains. Calorimetric analysis of the β -relaxation characteristics may be possible in analogy to the often performed analysis of the α -relaxation process, by following the evolution of enthalpy-recovery peaks on heating samples subjected to annealing at sufficiently low temperatures where α -relaxation is ceased [23,24]. Compared to mechanical and dielectric spectroscopy, such analyses,

however, are rare, probably due to difficulties in detecting the rather small changes in enthalpy and the limited heating-rate range to obtain information about activation energies from Arrhenius plots, when employing conventional differential scanning calorimetry (DSC).

Beside dedicated calorimetric β -relaxation studies on pharmaceuticals, [23,25] or metallic glasses, [26–34] also several reports about detection of endothermic sub- T_g annealing peaks on heating polymer glasses aged at low temperature are available [35–46]. However, their nature is not unequivocally discussed yet, as structural changes causing sub- T_g annealing peaks in calorimeter heating scans are discussed in terms of both glass relaxation, [35–42] and ordering processes [43–46]. Sub- T_g annealing peaks are documented for amorphous polymers including poly(vinyl chloride), [35] polyarylate, [36] polysulfone and polycarbonate, [37] as well as bulk and thin films of polystyrene, [38–40] which then are straightforward attributed to glass relaxation due to the inability for crystallization. In contrast, endothermic sub- T_g annealing peaks were also measured in crystallizable poly(ethylene terephthalate), [41–46] and associated to both relaxation and ordering. The ordering process is then discussed within the concept of cohesive entanglement, including “nematic interaction of neighboring chain segments” [44–46].

Recently, we investigated the low-temperature-mobility of molecular chain segments of polyamide 11 (PA 11) by means of calorimetry [47]. Motivation for this research was to understand the superior low-temperature toughness/impact strength of this polymer even at temperatures 80 K below T_g , [48] requiring the ability of amorphous molecule segments for local plastic flow in response to an external perturbation/load by absorption of energy rather than fracture [49,50]. The experiments successfully confirmed measurable changes of the local structure far below T_g , by detection of sub- T_g annealing peaks. Beside confirmation of the effects of annealing temperature and time on the amount of relaxation, [35] the study also showed that the related enthalpy changes (as a measure of the structure-relaxation process in the amorphous fraction) on low-temperature annealing—that is, annealing at temperatures $>(30-50)$ K below T_g —is independent on the presence of crystals. This observation was in strong contrast to analysis of relaxation close to T_g where cooperative large-amplitude motion in the amorphous phase is restricted in semicrystalline samples, with this result being in agreement with independent studies of the glass relaxation behavior of semicrystalline poly(L-lactic acid) [51,52]. A combined

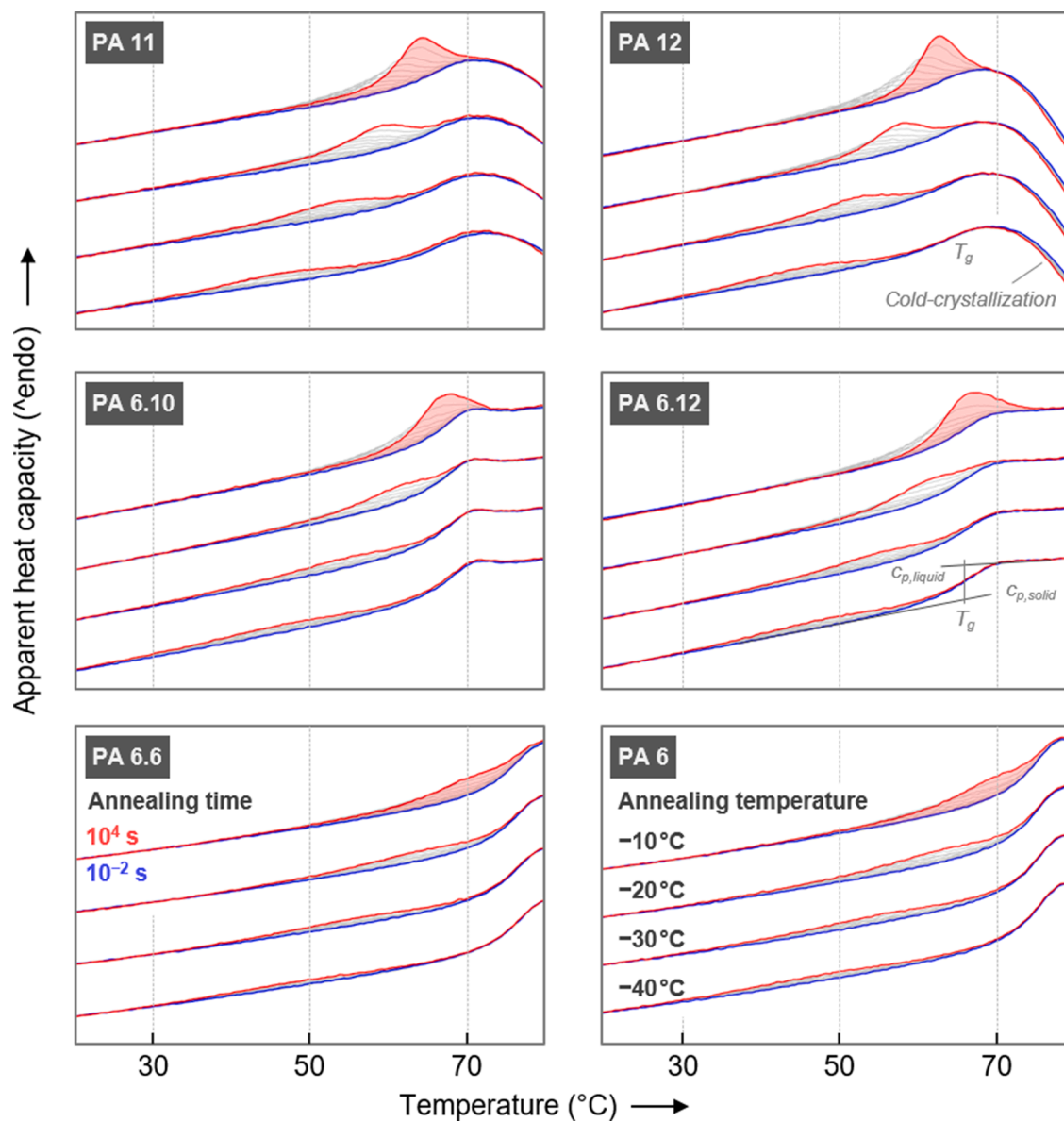


Fig. 2. FSC analysis heating scans (see Fig. 1), apparent heat capacity as a function of temperature, of low-temperature annealed polyamides as indicated. The four sets of curves refer to prior annealing at different temperatures between -40 and -10 °C (see bottom right plot), and blue and red coloring indicate annealing times of 10^{-2} and 10^4 s, respectively. Note that heating was performed to temperatures above the respective equilibrium melting temperatures according to Fig. 1, with the shown temperature interval selected for optimum representation of annealing peaks.

dielectric and calorimetric study on poly(ethylene terephthalate) revealed the absence of the large-amplitude motion in the rigid amorphous fraction while the intensity of the secondary β -relaxation scales with the crystal fraction only [53]. However, further details about the local low-temperature relaxation process in PA 11 are unknown, in particular which structural unit of the macromolecular chain contributes to the detected change of structure.

For this reason, in the present work a large set of aliphatic polyamides of different amide group concentration, implying different length of the methylene group sequence between the amide groups, is analyzed regarding changes of structure in the deep glassy state, using the same experimental strategy as applied in the PA 11 study [47]. As such, we follow the enthalpy change during isothermal annealing by analysis of the area of endothermic annealing peaks recorded subsequent to the annealing step. For both the approach of the annealing temperature, starting from the equilibrium liquid state, and the analysis heating scan, the use of fast scanning chip calorimetry (FSC) has been proven advantageous, as it allows precise preparation of glasses with a

specific cooling history, adjustment of annealing times down to sub-seconds related to the short instrument time constant, and analysis of weak transitions in the heating step, related to the fast heating capability [54].

2. Experimental

2.1. Materials

For gaining information about the effect of the amide group concentration in the molecular chains on changes of the physical structure during low-temperature annealing, a large set of different aliphatic polyamides was investigated. Table 1 provides a list of these polyamides including the source, grade, the structure of the chemical repeat unit, the number ratio of methylene and amide groups, and the glass transition temperature. Samples were available as pellets and used as-delivered.

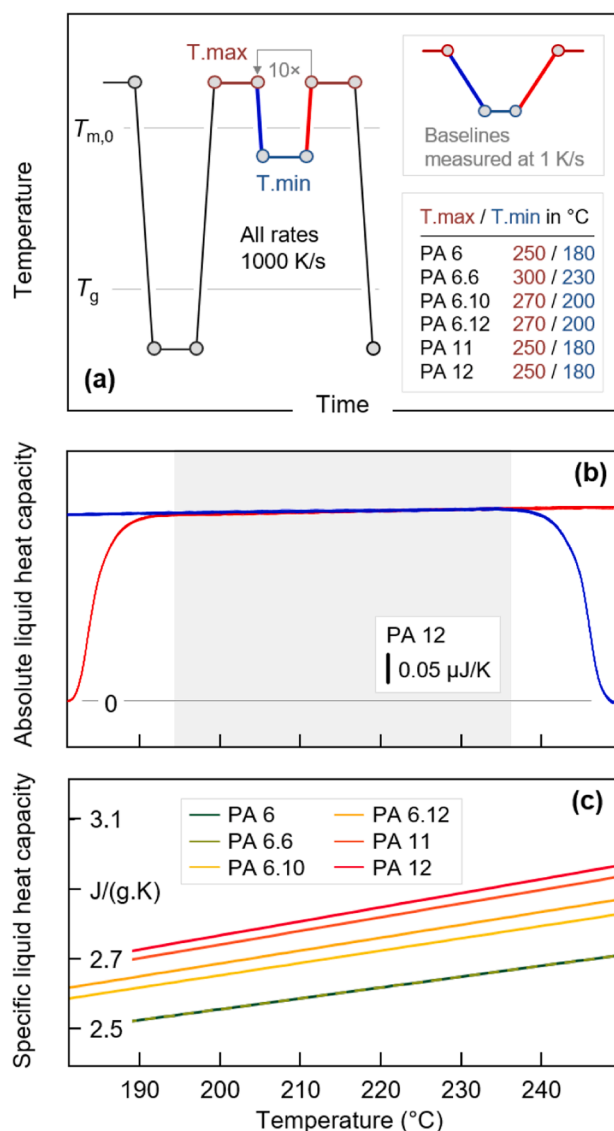


Fig. 3. (a) Temperature-time protocol for FSC analysis of the absolute heat capacity of polyamides in the liquid state, (b) example of FSC heating (red) and cooling scans (blue) obtained on PA 12, using the thermal profile of (a), and (c) specific liquid heat-capacity data of polyamides as available in the literature [66].

2.2. Instrumentation

For calorimetric analysis of structure changes in polyamides far below T_g , DSC of the Flash series were employed using conditioned and temperature-corrected UFS 1 chip sensors (Mettler-Toledo, Greifensee, Switzerland). The instruments were operated in conjunction with TC100 intracoolers (Huber, Offenbach, Germany), allowing to adjust the sample support temperature to -90 °C, and the sample environment was purged with nitrogen gas at a flow rate of 35 mL/min. Sample preparation included cutting of thin sections of 10 μm thickness with a microtome (Slee, Mainz, Germany), and limiting their lateral size to <100 μm with a scalpel under a stereomicroscope. Such specimens were then placed in the center of the heatable area of the sensor, where a homogeneous temperature distribution is expected [55]. We used both silicon oil and gold leaf as intermittent layers between the sensor membrane and the sample, to assure good thermal contact and minimize sensor-membrane bending due to different thermal expansion/contraction compared to the polymer samples, [56] affecting the instrumental baseline.

3. Results and discussion

Fig. 1 shows the temperature-time profile for FSC analysis of structure reorganization on annealing polyamides at temperatures far below the main glass transition temperature associated to the α -relaxation process. The equilibrium melt/liquid is cooled at a rate of 1000 K/s to temperatures between -10 and -40 °C, that is, to at least 50 K below T_g , and then annealed for periods of time between 10^{-2} to 10^4 s. The selected cooling rate of 1000 K/s is higher than the critical cooling required to suppress crystallization, reported for PA 6, 66, 11, and 12 in the literature, [57–61] or determined in this work. This implies that at the annealing temperature samples were fully amorphous. Subsequent the annealing step, samples were heated at a rate of 1000 K/s for analysis of possible changes of enthalpy.

Fig. 2 presents analysis heating scans of all polyamides investigated in the present work. Within the various plots, the four sets of curves refer to annealing experiments performed at -40 , -30 , -20 , and -10 °C, as indicated in the bottom right plot, and blue and red coloring indicate annealing for 10^{-2} and 10^4 s, respectively. For the annealing experiment performed at -10 °C (upper curve set in each plot), the difference in apparent heat capacity of samples annealed for 10^{-2} and 10^4 s is red-shaded. Note that cold-crystallization in the cases of PA 11 and PA 12 cannot be avoided at the selected heating rate of 1000 K/s, [60,61] with the observed exothermic peaks, however, not affecting data-analysis.

For all samples, endothermic annealing peaks are detected at temperatures well below T_g , with the latter recognized by the heat-capacity increment due to the solid-liquid transition and the different heat capacities of solid and liquid states, $c_{p,solid}$ and $c_{p,liquid}$, respectively, as illustrated with the gray lines in the center right-column plot [62]. The annealing peaks are rather broad and scale regarding their temperature and area with the annealing temperature and time, respectively, according to the expectations from the literature for both relaxation and ordering processes [35,44,63]. Important to note, the experiments of the present work are not designed to distinguish between these two causes of annealing peaks and therefore we generally express the observations as related to “changes of structure”. This notwithstanding, most striking, and being in foreground in the present study, however, is the detection of distinct differences in the amount of annealing-induced changes of structure in the various polyamides, as expressed by the different area of the annealing peaks obtained after annealing at identical conditions. This observation is obvious when comparing e.g. the red shaded area in the various plots, illustrating the difference of FSC heating curves/annealing-peak areas obtained after annealing the samples at -10 °C for 10^{-2} and 10^4 s. As such the peak area seems to follow the sequence [PA 6, PA 6.6] $<$ [PA 6.10, PA 6.12] $<$ [PA 11, PA 12], which, however, does not reflect the order of the glass transition temperatures as discussed in more detail below.

Quantitative comparison of the area of the endothermic low-temperature annealing peaks in terms of transition enthalpies requires normalization of absolute heat-flow rate data (in units of mW) or apparent heat capacities (in units of J/K) by the sample mass, which in FSC experiments is not directly obtained by weighting due to the small size of samples but only indirectly by internal calibration. In this work, we determined the sample mass by measurement of the absolute heat capacity in the melt state (in units of J/K) and comparison with the specific heat-capacity (in units of J/(g K)) available in the literature. For demonstration, Fig. 3a shows the used temperature-time protocol which includes a 10-cooling-and-heating loop in the temperature range from well above the equilibrium melting temperature $T_{m,0}$ (T_{max}) to slightly below $T_{m,0}$ (T_{min}), with more precise temperature-range information provided in the legend. Repeated scanning of the selected temperature interval served for excluding degradation and mass losses during measurement, while the selection of T_{min} slightly below $T_{m,0}$ is considered uncritical for determination of the liquid-phase heat capacity, since crystallization sets in only at significantly lower temperature at the

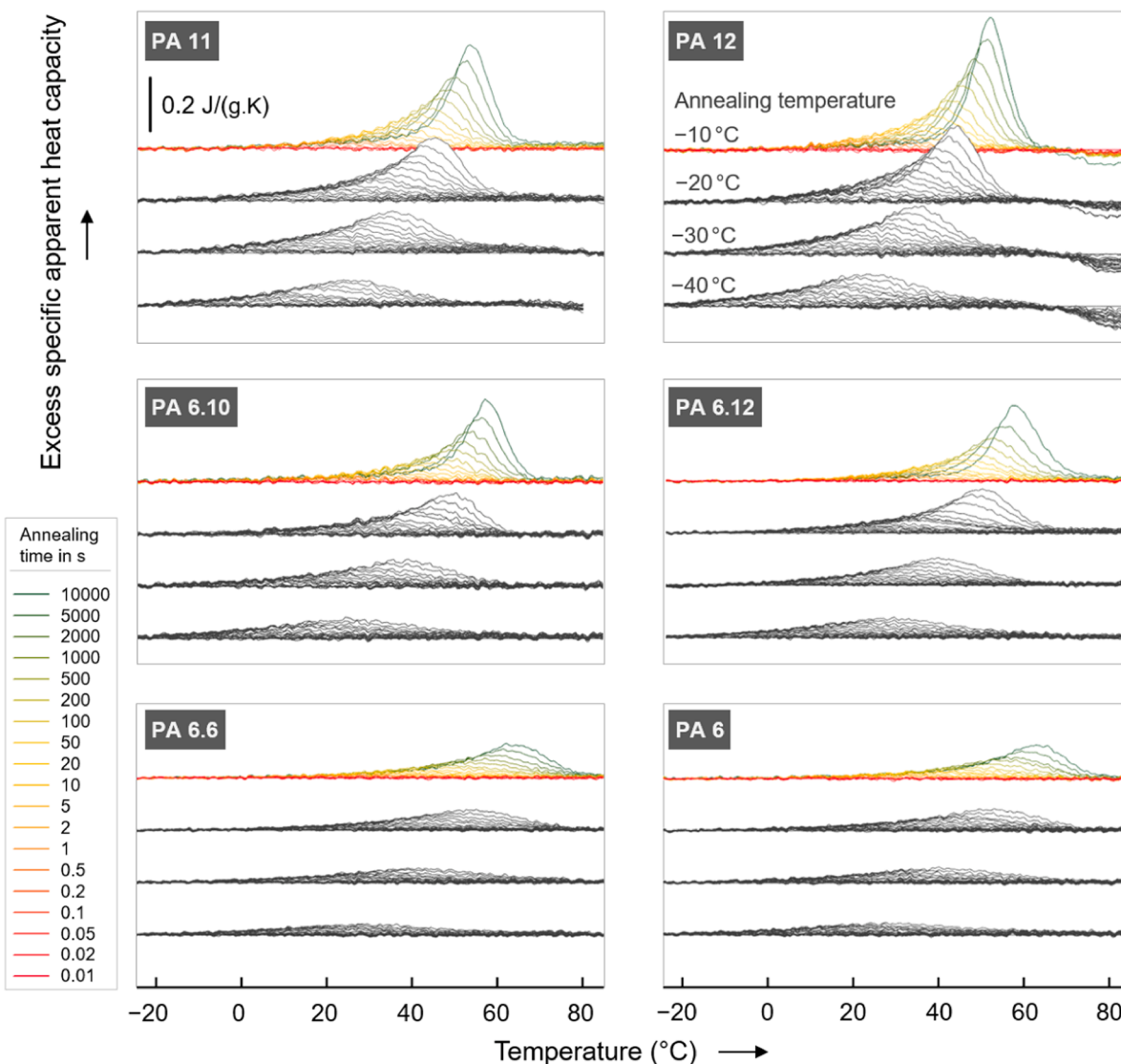


Fig. 4. Low-temperature-annealing-caused excess specific apparent heat capacity of different polyamides as a function of temperature. Samples were annealed at temperatures between -40 (lower set of curves in each plot) and -10 °C (upper set of curves in each plot) for different periods of time between 10^{-2} and 10^4 s (see legend).

selected cooling rate of 1000 K/s. Heat-flow-raw data were corrected for instrumental heat losses estimated by a baseline recorded using a rate of 1 K/s, as indicated in the legend [64,65]. As an example of baseline-corrected data, Fig. 3b presents sets of cooling (blue) and heating scans (red), recorded between 180 and 250 °C obtained on PA 12, revealing the initial approach of instrumental steady state when starting to cool/heat the sample after the isothermal segment at T_{max}/T_{min} . Within the gray-shaded temperature-range, the system is in steady state, allowing to interpret the data as heat capacities. Finally, for estimation of the sample mass, measured absolute heat capacities are compared with specific heat-capacity data of the liquid phase available in the literature, [66] shown in Fig. 3c. As such, sample masses were between about 120 and 220 ng, with the rather large sample size being advantageous for the detection of the relatively low amount of enthalpy changes during the low-temperature annealing steps. With the knowledge of the sample mass, a quantitative comparison of the above proposed different behavior of the various polyamides becomes possible.

Fig. 4 shows with the various plots sample-mass-normalized excess apparent heat capacities of the different polyamides of Table 1 as a function of temperature, caused by prior isothermal annealing at temperatures between -40 (lower set of curves in each plot) and -10 °C

(upper set of curves in each plot) for different periods of time between 10^{-2} and 10^4 s (see legend). These data confirm the initial suggestion that low-temperature-annealing-caused enthalpy changes, and therefore changes of structure, for given conditions of thermal treatment, depend on the specific chemical structure of the polyamide, being smallest for PA 6 and PA 6.6, and largest for PA 11 and PA 12.

Further quantification of the amount of changes of structure on low-temperature annealing is then done by integration of the observed peaks, and plotting the area in units of J/g as a function of the annealing time, as shown with Fig. 5. The lower part of the Figure is organized such that data associated to specific polyamides and annealing temperatures are presented separately, with the main information that for all polyamides structure-equilibration begins latest after about 10^0 s, does not complete within 10^4 s, and is more pronounced on annealing at higher temperature (see red curves). Since a comparison of the annealing behavior of the various polyamides is difficult when data sets are vertically shifted for improved illustration of the effect of the annealing temperature, in the upper part of the figure all curves are presented superimposed, for highlighting the effect of the different chemical structure of the various polyamides. While for PA 6 and PA 6.6, annealing for 10^4 s leads to changes of structure equivalent to a change

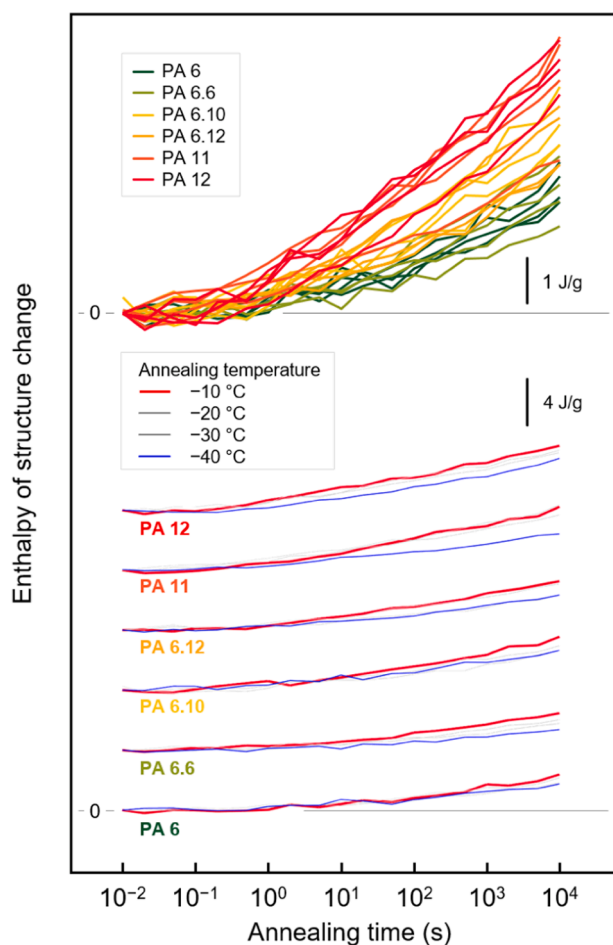


Fig. 5. Enthalpy of structure-change during low-temperature annealing of different polyamides, calculated by the area of annealing peaks shown in Fig. 4, as a function of the annealing time. In the lower part, data associated to specific polyamides are vertically shifted for improved visibility, while in the upper part all curves are superimposed.

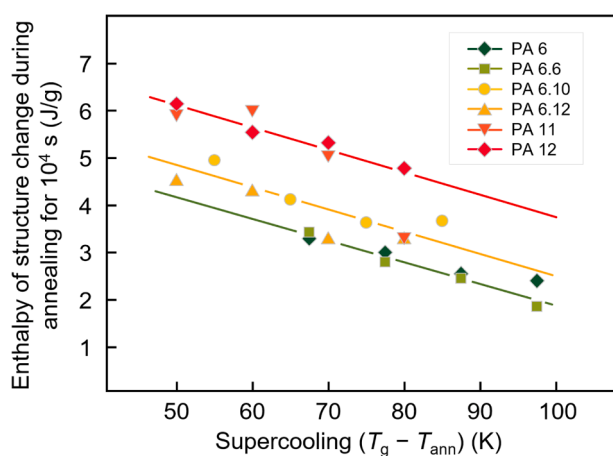


Fig. 6. Enthalpy of structure-change during low-temperature annealing of different polyamides for 10^4 s as a function of the temperature difference between T_g , measured on cooling at 1000 K/s, and the annealing temperature T_{ann} (supercooling). Lines serve for guiding the eye only.

of enthalpy of about 2 J/g, it is about twice for PA 11 and PA 12. The latter result quantitatively confirms data observed on PA 11 in an earlier independent study [47].

Since the process of structure equilibration on low-temperature annealing does not complete within the maximum annealing/measurement time, and since the data do not allow a prediction of an equilibrium/plateau value, we employed the enthalpy-change during annealing for 10^4 s for benchmarking the different low-temperature structure-equilibration strength of the various polyamides. As such, Fig. 6 shows for the different polyamides the enthalpy-change during low-temperature structure equilibration for 10^4 s as a function of the temperature difference between T_g and the annealing temperature T_{ann} , denoted as degree of supercooling the thermodynamically unstable system below T_g . The reason for not plotting the enthalpy change directly as a function of the annealing temperature T_{ann} is the observation of different glass transition temperatures for the various polyamides (PA 6 and PA 6.6: 57.5 °C, PA 6.10: 45 °C, PA 6.12, PA 11, and PA 12: 40 °C), showing a similar trend as in the literature, [67] decreasing with increasing length of the methylene-sequence between amide groups. In other words, at a selected constant annealing temperature, the glasses of the different polyamides exhibit different mobility of structural units, controlling the kinetics of structure reorganization.

The data of Fig. 6 confirm the initial qualitative evaluation of the experimental raw data of Fig. 2. First, there is observed a significant decrease of the enthalpy at temperatures lower than required for α -relaxation [$T < (T_g - 50$ K)], which, though fading with decreasing absolute temperature, is still large at a temperature 100 K below T_g . Second, and more important regarding the scope of this study, the change of enthalpy, that is, the amount of structure reorganization at a given glass-supercooling condition depends on the chemical structure of the polyamide repeat unit: the longer the methylene-sequence between amide groups, as e.g. expressed as number ratio between the CH_2 and CO-NH groups (see right column in Table 1), the more pronounced are the changes of structure deep in the glassy state. Conclusions whether the decrease of the enthalpy is caused by a relaxation of the glass (enthalpy relaxation), involving non-cooperative conformational changes of sub-nm sized units without ordering, or by local ordering processes (crystallization), that is, formation of small ordered domains with enthalpic interactions between neighbored units, cannot be drawn from the performed experiments. Therefore the observed enthalpy changes, throughout this study, are denoted as (local) structure reorganization only. In any case, enthalpy relaxation and formation of a glass of lower (free) enthalpy, or formation of ordered structures (probably not fulfilling the prerequisites to be classified as a classical phase) [68] with a lower free enthalpy than the surrounding non-ordered phase, is enhanced if the concentration of amide groups in the macromolecular chains is low. A possible reason is that the hydrogen bonds connect to neighbored chain segments and generate a three-dimensional network, [69,70] therefore perhaps reducing also the mobility of the methylene-sequences in between, slowing down their relaxation/ordering. A similar picture has been developed for the “classical” above- T_g -crystallization process, for which the relatively fast crystallization process of PA 10.12 and PA 12 is associated to low hydrogen-bond density, supporting short-range diffusion in the low-temperature region slightly above T_g [71]. This experimental observation, in addition, was confirmed by molecular simulation with the main outcome that strong hydrogen-bonding slows down polymer diffusion [72]. Worth noting that the suggested reduced (local, segmental) mobility of polyamides with high hydrogen-bond density is in agreement with their lower heat capacity (in units of J/(g.K)) in both the liquid (see also Fig. 3c) and solid states (e.g. at 270 K), [66,73] which, however, does not imply a lowered relaxation strength as judged by the heat-capacity step at T_g ($\Delta c_p|_{T=T_g}$). For PA 6 and PA 12, $\Delta c_p|_{T=T_g}$ -values of 0.48 and 0.38 J/(g.K) are reported, [66] respectively, and for this reason, the smaller annealing peaks in the case of PA 6, compared to those of PA 12, obtained at comparable annealing conditions, cannot be explained by an inherently reduced relaxation capacity,

if caused by glass relaxation.

4. Conclusion

In the present work, physical aging and structure-reorganization/equilibration of non-crystallized aliphatic polyamides at temperatures far (50–100 K) below T_g , that is, at temperatures where α -relaxation is largely suppressed, has been detected by calorimetry via analysis of endothermic annealing peaks in heating scans recorded subsequent the low-temperature equilibration step. Annealing aliphatic polyamides at such low temperature causes a decrease of the enthalpy of the order of magnitude of a few J/g, increasing with time and temperature of annealing. Such enthalpy-changes are typical for both relaxation and ordering processes. Systematic variation of the chemical structure of the repeat unit of the investigated aliphatic polyamides allowed linking the magnitude of the structure-equilibration process to the length of the methylene sequence between amide groups, such that structure equilibration is enhanced in polyamides with longer methylene sequences in their repeat unit. In other words, the obtained experimental data provide evidence that with increasing density of the hydrogen bond network, connecting neighbored chain segments, relaxation and/or ordering processes are slowing down and hindered.

CRedit authorship contribution statement

René Androsch: Writing – review & editing, Writing – original draft, Investigation, Funding acquisition, Conceptualization. **Christoph Schick:** Writing – review & editing, Conceptualization.

Declaration of competing interest

The authors declare that they have no known competing financial interests or personal relationships that could have appeared to influence the work reported in this paper.

Acknowledgment

The project is funded by the Deutsche Forschungsgemeinschaft (DFG, German Research Foundation)-Projektnummer 464908856.

Data availability

Data will be made available on request.

References

- J.D. Ferry, *Viscoelastic Properties of Polymers*, John Wiley & Sons, New York, NY, USA, 1980.
- G. Adam, J.H. Gibbs, On the temperature dependence of cooperative relaxation properties in glass-forming liquids, *J. Chem. Phys.* 43 (1965) 139–146.
- L. Larini, A. Ottochian, C. De Michele, D. Leporini, Universal scaling between structural relaxation and vibrational dynamics in glass-forming liquids and polymers, *Nat. Phys.* 4 (2008) 42.
- E.D. Zanoatto, J.C. Mauro, The glassy state of matter: its definition and ultimate fate, *J. Non-Cryst. Solids* 471 (2017) 490–495.
- I.M. Hodge, Enthalpy relaxation and recovery in amorphous materials, *J. Non-Cryst. Solids* 169 (1994) 211–266.
- C.A. Angell, K.L. Ngai, G.B. McKenna, P.F. McMillan, S.W. Martin, Relaxation in glass forming liquids and amorphous solids, *J. Appl. Phys.* 88 (2000) 3113–3157.
- J. Zhao, S.L. Simon, G.B. McKenna, Using 20-million-year-old amber to test the super-arrhenius behaviour of glass-forming systems, *Nat. Comm.* 4 (2013) 1783.
- D. Rigby, R.J. Roe, Molecular dynamics simulation of polymer liquid and glass. I. Glass transition, *J. Chem. Phys.* 87 (1987) 7285–7292.
- L.C.E. Struik, Volume relaxation in polymers, *Rheol. Acta* 5 (1966) 303–311.
- G.T. Davis, R.K. Eby, Glass transition of polyethylene: volume relaxation, *J. Appl. Phys.* 44 (1973) 4274–4281.
- K. Adachi, T. Kotaka, Volume and enthalpy relaxation in polystyrene, *Polym. J.* 14 (1982) 959–970.
- I.M. Hodge, Physical aging in polymer glasses, *Science* 267 (1995) 1945–1947.
- J.M. Hutchinson, S. Smith, B. Horne, G.M. Gourlay, Physical aging of polycarbonate: enthalpy relaxation, creep response, and yielding behavior, *Macromolecules* 32 (1999) 5046–5061.
- H.M.N. Iqbal, C. Sungkapreecha, R. Androsch, Enthalpy relaxation of the glass of poly(L-lactic acid) of different D-isomer content and its effect on mechanical properties, *Polym. Bull.* 74 (2017) 2565–2573.
- H. Zhou, E.A. Lofgren, S.A. Jabarin, Effects of microcrystallinity and morphology on physical aging and its associated effects on tensile mechanical and environmental stress cracking properties of poly(ethylene terephthalate), *J. Appl. Polym. Sci.* 112 (2009) 2906–2917.
- A. Aref-Azar, F. Biddlestone, J.N. Hay, R.N. Haward, The effect of physical ageing on the properties of poly(ethylene terephthalate), *Polymer* 24 (1983) 1245–1251.
- G.R. Garrett, M.D. Demetriou, M.E. Launey, W.L. Johnson, Origin of embrittlement in metallic glasses, *Proc. Nat. Acad. Sci.* 113 (2016) 10257–10262.
- Q. Yang, S.-X. Peng, Z. Wang, H.-B. Yu, Shadow glass transition as a thermodynamic signature of β relaxation in hyper-quenched metallic glasses, *Nat. Sci. Rev.* 7 (2020) 1896–1905.
- E. Donth, Characteristic length of the glass transition, *J. Polym. Sci. Polym. Phys.* 34 (1996) 2881–2892.
- E. Donth, *The Glass transition: Relaxation dynamics in Liquids and Disordered Materials*, Springer, Berlin, 2013.
- T. Kawaguchi, The dynamic mechanical properties of nylons, *J. Appl. Polym. Sci.* 2 (1959) 56–61.
- V. Frosini, E. Butta, Some remarks on the mechanical relaxations in aliphatic, partially aromatic and wholly aromatic polyamides, *J. Polym. Sci. Polym. Letters* 9 (1971) 253–260.
- S. Vyazovkin, I. Dranca, Probing beta relaxation in pharmaceutically relevant glasses by using DSC, *Pharm. Res.* 23 (2006) 422–428.
- V.A. Bershtein, V.M. Egorov, *Differential Scanning Calorimetry of Polymers: Physics, Chemistry, Analysis, Technology*, Ellis Horwood, 1994.
- J. Fan, E.I. Cooper, C.A. Angell, Glasses with strong calorimetric beta-glass transitions and the relation to the protein glass transition problem, *J. Phys. Chem.* 98 (1994) 9345–9349.
- H.S. Chen, A. Inoue, T. Masumoto, Two-stage enthalpy relaxation behaviour of (Fe_{0.5}Ni_{0.5})₈₃P₁₇ and (Fe_{0.5}Ni_{0.5})₈₃B₁₇ amorphous alloys upon annealing, *J. Mater. Sci.* 20 (1985) 2417–2438.
- D.P.B. Aji, G.P. Johari, Kinetic-freezing and unfreezing of local-region fluctuations in a glass structure observed by heat capacity hysteresis, *J. Chem. Phys.* 142 (2015) 214501.
- D.V. Louzguine-Luzgin, I. Seki, T. Yamamoto, H. Kawaji, C. Suryanarayana, A. Inoue, Double-stage glass transition in a metallic glass, *Phys. Rev. B* 81 (2010) 144202.
- I. Gallino, D. Cangialosi, Z. Evenson, L. Schmitt, S. Hechler, M. Stolpe, B. Ruta, Hierarchical aging pathways and reversible fragile-to-strong transition upon annealing of a metallic glass former, *Acta Mater.* 144 (2018) 400–410.
- L. Song, W. Xu, J. Huo, J.Q. Wang, X. Wang, R. Li, Two-step relaxations in metallic glasses during isothermal annealing, *Intermetallics* 93 (2018) 101–105.
- M. Gao, J.H. Perepezko, Separating β relaxation from α relaxation in fragile metallic glasses based on ultrafast flash differential scanning calorimetry, *Phys. Rev. Mater.* (4) (2020) 025602.
- M.W. da Silva Pinto, L. Daum, H. Rösner, G. Wilde, Correlations between shadow glass transition, enthalpy recovery and medium range order in a Pd₄₀Ni₄₀P₂₀ bulk metallic glass, *Acta Mater.* 275 (2024) 120034.
- Q. Sun, W. Wang, M. Huang, X. Zhao, J. Lv, G. Zhang, L. Liu, J. Yi, Probing the decoupling degree between α and β relaxations in metallic glasses through differential scanning calorimetry, *J. Non-Cryst. Sol.* 641 (2024) 123089.
- R. Zhao, H.Y. Jiang, P. Luo, L.Q. Shen, P. Wen, Y.H. Sun, H.Y. Bai, W.H. Wang, Reversible and irreversible β -relaxations in metallic glasses, *Phys. Rev. B* 101 (2020) 094203.
- A.R. Berens, I.M. Hodge, Effects of annealing and prior history on enthalpy relaxation in glassy polymers. 1. Experimental study on poly(vinyl chloride), *Macromolecules* 15 (1982) 756–761.
- N.G. Perez-De Eulate, D. Cangialosi, The very long-term physical aging of glassy polymers, *Phys. Chem. Chem. Phys.* 20 (2018) 12356–12361.
- H.S. Chen, T.T. Wang, Sub-sub T_g structural relaxation in glassy polymers, *J. Appl. Phys.* 52 (1981) 5898–5902.
- V.M. Boucher, D. Cangialosi, A. Alegría, J. Colmenero, Reaching the ideal glass transition by aging polymer films, *Phys. Chem. Chem. Phys.* 19 (2017) 961–965.
- V.M. Boucher, D. Cangialosi, A. Alegría, J. Colmenero, Complex nonequilibrium dynamics of stacked polystyrene films deep in the glassy state, *J. Chem. Phys.* 146 (2017) 203312.
- D. Cangialosi, V.M. Boucher, A. Alegría, J. Colmenero, Direct evidence of two equilibration mechanisms in glassy polymers, *Phys. Rev. Lett.* 111 (2013) 095701.
- M.R. Tant, G.L. Wilkes, Physical aging studies of semicrystalline poly(ethylene terephthalate), *J. Appl. Polym. Sci.* 26 (1981) 2813–2825.
- G. Vigier, J. Tatibouet, Physical ageing of amorphous and semicrystalline poly(ethylene terephthalate), *Polymer* 34 (1993) 4257–4266.
- R. Hagege, Ageing behavior of pre-oriented PET yarns, followed by DSC, *Text. Res. J.* 47 (1977) 229–231.
- R. Qian, D. Shen, F. Sun, L. Wu, The effects of physical ageing on conformational changes of poly(ethylene terephthalate) in the glass transition region, *Macromol. Chem. Phys.* 197 (1996) 1485–1493.
- R. Qian, The concept of cohesive entanglement, *Macromol. Symp.* 124 (1977) 15–26.
- Y. Wang, D. Shen, R. Qian, Subglass-transition-temperature annealing of poly(ethylene terephthalate) studied by FTIR, *J. Polym. Sci. Part B: Polym. Phys.* 36 (1998) 783–788.

- [47] R. Androsch, K. Jariyavidyanont, C. Schick, Enthalpy relaxation of polyamide 11 of different morphology far below the glass transition temperature, *Entropy* 21 (2019) 984.
- [48] Key Properties of Rilsan® PA11. Available online: <https://hpp.arkema.com/en/product-families/rilsan-polyamide-11-resins/key-properties/> (accessed on 27 February 2025).
- [49] A.S. Argon, R.E. Cohen, Toughenability of polymers, *Polymer* 44 (2003) 6013–6032.
- [50] W.G. Perkins, Polymer toughness and impact resistance, *Polym. Eng. Sci.* 39 (1999) 2445–2460.
- [51] M.C. Righetti, E. Mele, Structural relaxation in PLLA: contribution of different scale motions, *Thermochim. Acta* 672 (2019) 157–161.
- [52] R. Zhang, K. Jariyavidyanont, E. Zhuravlev, C. Schick, R. Androsch, Physical aging and glass transition dynamics of semicrystalline poly(lactic acid) for 3D-printing applications investigated by fast scanning calorimetry, *Macromolecules* 57 (2023) 32–41.
- [53] C. Schick, J. Dobberty, M. Potter, H. Dehne, A. Hensel, A. Wurm, A.M. Ghoneim, S. Weyer, Separation of components of different molecular mobility by calorimetry, dynamic mechanical and dielectric spectroscopy, *J. Therm. Anal.* 49 (1997) 499–511.
- [54] C. Schick, V. Mathot, *Fast Scanning Calorimetry*, Springer, Cham, 2016.
- [55] K. Jariyavidyanont, A. Abdelaziz, R. Androsch, C. Schick, Experimental analysis of lateral thermal inhomogeneity of a specific chip-calorimeter sensor, *Thermochim. Acta* 674 (2019) 95–99.
- [56] A. Wurm, A. Herrmann, M. Cornelius, E. Zhuravlev, D. Pospiech, R. Nicula, C. Schick, Temperature dependency of nucleation efficiency of carbon nanotubes in PET and PBT, *Macromol. Mater. Eng.* 300 (2015) 637–649.
- [57] R. Androsch, C. Schick, J.W.P. Schmelzer, Sequence of enthalpy relaxation, homogeneous crystal nucleation and crystal growth in glassy polyamide 6, *Eur. Polym. J.* 53 (2014) 100–108.
- [58] A.M. Rhoades, J.L. Williams, R. Androsch, Crystallization kinetics of polyamide 66 at processing-relevant cooling conditions and high supercooling, *Thermochim. Acta* 603 (2015) 103–109.
- [59] A. Mollova, R. Androsch, D. Mileva, C. Schick, A. Benhamida, Effect of supercooling on crystallization of polyamide 11, *Macromolecules* 46 (2013) 828–835.
- [60] R. Zhang, K. Jariyavidyanont, M. Du, E. Zhuravlev, C. Schick, R. Androsch, Nucleation and crystallization kinetics of polyamide 12 investigated by fast scanning calorimetry, *J. Polym. Sci.* 60 (2022) 842–855.
- [61] K. Jariyavidyanont, E. Zhuravlev, C. Schick, R. Androsch, Kinetics of homogeneous crystal nucleation of polyamide 11 near the glass transition temperature, *Polym. Cryst.* 4 (2021) e10149.
- [62] B. Wunderlich, The heat capacity of polymers, *Thermochim. Acta* 300 (1997) 43–65.
- [63] C. Schick, R. Androsch, The origin of annealing peaks in semicrystalline polymers: enthalpy recovery or melting? *Macromolecules* 53 (2020) 8751–8756.
- [64] E. Zhuravlev, C. Schick, Fast scanning power compensated differential scanning nano-calorimeter: 2. Heat capacity analysis, *Thermochim. Acta* 505 (2010) 14–21.
- [65] J.E. Schawe, S. Pogatscher, Material characterization by fast scanning calorimetry: practice and applications, in: C. Schick, V. Mathot (Eds.), *Fast Scanning Calorimetry*, Springer, 2016, pp. 3–80.
- [66] A. Xenopoulos, B. Wunderlich, Thermodynamic properties of liquid and semicrystalline linear aliphatic polyamides, *J. Polym. Sci. Polym. Phys.* 28 (1990) 2271–2290.
- [67] R. Greco, L. Nicolais, Glass transition temperature in nylons, *Polymer* 17 (1976) 1049–1053.
- [68] B. Wunderlich, Thermodynamics and properties of nanophases, *Thermochim. Acta* 492 (2009) 2–15.
- [69] L.R. Schroeder, S.L. Cooper, Hydrogen bonding in polyamides, *J. Appl. Phys.* 47 (1976) 4310–4317.
- [70] N.S. Murthy, Hydrogen bonding, mobility, and structural transitions in aliphatic polyamides, *J. Polym. Sci. Polym. Phys.* 44 (2006) 1763–1782.
- [71] X. Li, Y. He, X. Dong, X. Ren, H. Gao, W. Hu, Effects of hydrogen-bonding density on polyamide crystallization kinetics, *Polymer* 189 (2020) 122165.
- [72] J. Zhang, W. Hu, Roles of specific hydrogen-bonding interactions in the crystallization kinetics of polymers, *Polymer* 283 (2023) 126278.
- [73] A. Xenopoulos, B. Wunderlich, Heat capacities of solid polyamides, *Polymer* 31 (1990) 1260–1268.